Eur. Phys. J. A (2017) **53**: 81
DOI 10.1140/epja/i2017-12265-x

THE EUROPEAN PHYSICAL JOURNAL A

Regular Article – Theoretical Physics

Jet-dilepton conversion from an anisotropic quark-gluon plasma

Arghya Mukherjee[a], Mahatsab Mandal, and Pradip Roy

Saha Institute of Nuclear Physics, 1/AF Bidhannagar Kolkata - 700064, India

Received: 8 November 2016 / Revised: 14 March 2017
Published online: 2 May 2017 – © Società Italiana di Fisica / Springer-Verlag 2017
Communicated by H. Wittig

Abstract. We calculate the yield of lepton pair production from jet-plasma interaction where the plasma is anisotropic in momentum space. We compare both the M and p_T distributions from such process with the Drell-Yan contribution. It is observed that the invariant mass distribution of the lepton pair from such process dominates over the Drell-Yan one up to 3 GeV at RHIC and up to 10 GeV at LHC. Moreover, it is found that the contribution from the anisotropic quark gluon plasma (AQGP) increases marginally compared to the isotropic QGP. In case of p_T-distribution we observe an increase by a factor of 3–4 in the entire p_T-range at RHIC for AQGP. However, at LHC the change in the p_T-distribution is marginal as compared to the isotropic case. It should be noted that we have used a two stage evolution scenario. First, the system evolves with pre-equilibrium state anisotropy up to τ_{iso} (the isotropization time). After that the system evolves hydrodynamically.

1 Introduction

The primary goal of heavy-ion collisions at the Relativistic Heavy Ion Collider (RHIC) at BNL and at the Large Hadron Collider (LHC) at CERN is to establish the existence of a transient phase consisting of quarks, anti-quarks and gluons known as Quark Gluon Plasma (QGP). Since such a phase lasts for a few fm/c, it is impossible to observe it directly. Thus, various probes have been proposed in the literature [1–11]. The electromagnetic probe is one of them. The advantage of such probe is that once these are produced they can escape the interaction zone without much distortion in their energy and momentum. They, thus carry the information of the collision dynamics very effectively. Photons and dileptons are produced throughout the evaluation process of the collisions. In the low and intermediate mass region, lepton pairs are produced from various microscopic processes such as $q\bar{q} \to l^+l^-$, virtual Compton process ($qg \to q\gamma^*$) etc. and also from various hadronic reactions and decays. In the high-mass region, there is the contribution from the Drell-Yan process, which can be calculated from pQCD. Another important contribution in this invariant-mass region is the jet-dilepton conversion in the QGP. Several authors [12–15] have estimated this contribution where a jet quark (anti-quark) interacts with a thermal anti-quark (quark) to produce a large-mass lepton pair. It should be noted that gluon jets would also give rise to dilepton through the process $q\,g \to q\,\gamma^*$. But from the phase space consideration it is not favoured over the process considered here. In a previous calculation, it is found that the contribution from the gluon jets is sub-leading [8]. Thus, in this work, we shall consider only the annihilation process due to quark jets. It should further be noted that before annihilation of a q ($\bar{q}$) jet with a thermal $\bar{q}$ (q), the q ($\bar{q}$) jet may lose energy. Such possibility has also been considered in refs. [13–15]. It has been observed in all those calculations that the magnitude of this mechanism is orders of magnitude larger than the thermal processes and is of the same order of the Drell-Yan processes [16]. It is to be noted that in all those calculations an isotropic plasma has been assumed to be formed. But the most difficult problem lies in the determination of isotropization and thermalization time scales ($\tau_{\rm iso}$ and $\tau_{\rm therm}$) of the QGP. Studies on elliptic flow (up to about $p_T \sim 1.52$ GeV) using ideal hydrodynamics indicate that the matter produced in such collisions becomes isotropic with $\tau_{\rm iso} \sim 0.6$ fm/c [17]. On the contrary, perturbative estimates yield much slower thermalization of QGP [18–20]. However, recent hydrodynamical studies [21] have shown that due to the poor knowledge of the initial conditions, there is a sizable amount of uncertainty in the estimation of thermalization or isotropization time. Thus it is necessary to find suitable probes which are sensitive to the initial temperature. As mentioned earlier electromagnetic probes have long been considered to be one of the most promising tools to characterize the initial state of the collisions [6–9, 11]. Dileptons (photon as well) can be one such observables. In the early stages of heavy ion collisions, due to the rapid longitudinal expansion the plasma after formation in isotropic phase, may

[a] e-mail: arghya.mukherjee@saha.ac.in

become anisotropic [22–30]. As a result the momentum distribution of the plasma particles become anisotropic in momentum space. The author in ref. [31] have calculated the "medium" dilepton yield for various isotropization times and compared it with Drell-Yan and jet-thermal processes. It is shown that the effect of the anisotropy cannot be neglected while calculating M-distribution and p_T-distribution. In fact in certain kinematic region this contribution is comparable to Drell-Yan as well as jet-thermal process. Jet-photon conversion in the AQGP has been calculated in ref. [32] with p_T up to 14 GeV to extract the isotropization time. Also in intermediate and low p_T the photon transverse momentum distribution has been calculated to infer about the isotropization time scale [33]. It is to be noted that the extracted values of $\tau_{\rm iso}$ from the above two cases are consistent. To the best of our knowledge, the contribution of the jet-dilepton conversion in AQGP has not been done so far. It is, thus, our purpose to estimate the dilepton yield from jet-plasma interaction in the present work. It should be noted here that we restrict ourselves to the QGP phase and stop the hydrodynamic evolution before the cross-over as the high mass dileptons originate mainly from the QGP phase. To keep the things simple, in this work, we shall not include the energy loss of the jet in the AQGP.

It should be noted that in absence of any precise knowledge about the dynamics at early time of the collision, one can introduce phenomenological models to describe the evolution of the pre-equilibrium phase. In this work, we will use one such model, proposed in ref. [31, 34, 35], for the time dependence of the anisotropy parameter, $\xi(\tau)$, and hard momentum scale, $p_{\rm hard}(\tau)$. This model introduces four parameters to parameterize the ignorance of pre-equilibrium dynamics: the parton formation time (τ_i), the isotropization time ($\tau_{\rm iso}$), which is the time when the system starts to undergo ideal hydrodynamical expansion and γ sets the sharpness of the transition to hydrodynamical behavior. The fourth parameter δ is introduced to characterize the nature of pre-equilibrium anisotropy, *i.e.* whether the pre-equilibrium phase is non-interacting or collisionally broadened.

The plan of the paper is the following. In the next section we describe the formalism of jet-conversion dilepton production in AQGP. Jet-production and Drell-Yan process will be discussed in sect. 3. We present a brief discussion on space-time evolution of AQGP in sect. 4. Section 5 will be devoted to present the results. Finally, we summarize in sect. 6.

2 Formalism

According to the relativistic kinetic theory, the dilepton production rate at leading order in the coupling α, is given by [11, 36, 37]

$$\frac{{\rm d}R^{l^+l^-}}{{\rm d}^4P} = \int \frac{{\rm d}^3\mathbf{p}_1}{(2\pi)^3}\frac{{\rm d}^3\mathbf{p}_2}{(2\pi)^3} f_{q/\bar{q}}(\mathbf{p}_1) f_{\rm jet}(\mathbf{p}_2)\, v_{12}\, \sigma^{l^+l^-}_{q\bar{q}} \times \delta^{(4)}(P - p_1 - p_2), \tag{1}$$

where $f_{\rm jet}$ and $f_{q/\bar{q}}$ are the phase space distribution of the jet quarks/anti-quarks and medium quarks/anti-quarks respectively. The total cross section of the $q\bar{q} \to l^+l^-$ interaction is given by

$$\sigma^{l^+l^-}_{q\bar{q}} = \frac{4\pi}{3}\frac{\alpha^2}{M^2} N_c N_s \left(1 + \frac{2m_l^2}{M^2}\right)\left(1 - \frac{4m_l^2}{M^2}\right)^{1/2} \sum_q e_q^2, \tag{2}$$

where $N_c(=3)$ and $N_s(=2)$ are the color factor and spin factor, respectively and $\sum_q e_q^2 = \frac{5}{9}$ for two flavours u and d. m_l is the mass of lepton and M is the invariant mass of the lepton pair which is much greater than the lepton mass. So we can easily ignore the lepton mass and we find $\sigma^{l^+l^-}_{q\bar{q}} = \frac{4\pi\alpha^2}{3M^2} N_c N_s \sum_q e_q^2$. We also assume that the distribution functions of quarks and anti-quarks are the same. v_{12} is the relative velocity between the jet quark and medium quark/anti-quark:

$$v_{12} = \frac{(p_1 + p_2)^2}{2E_1E_2}\,. \tag{3}$$

In this work we consider the medium is anisotropic in momentum space so that the anisotropic distribution function can be obtained from an arbitrary isotropic distribution by squeezing or stretching along the preferred direction in the momentum space [23]:

$$f_{q/\bar{q}}(\mathbf{p}, \xi, p_{\rm hard}) = f_{q/\bar{q}}\left(\sqrt{\mathbf{p}^2 + \xi(\tau)(\mathbf{p}\cdot\hat{\mathbf{n}})^2}, p_{\rm hard}(\tau)\right), \tag{4}$$

where $\hat{\mathbf{n}}$ is the direction of anisotropy, $p_{\rm hard}(\tau)$ is a time-dependent hard momentum scale and $\xi(\tau)$ is a time-dependent parameter reflecting the strength of the momentum anisotropy. In isotropic case, where $\xi = 0$, $p_{\rm hard}$ can be recognized with the plasma temperature T.

The phase space distribution function for a jet, assuming the constant transverse density of the nucleus is given by [13, 38]

$$f_{\rm jet}(\mathbf{p}) = \frac{(2\pi)^3}{g_q}\frac{\mathcal{P}(|\boldsymbol{\omega}_r|)}{\sqrt{\tau_i^2 - z_0^2}}\frac{1}{p_T}\frac{{\rm d}N_{\rm jet}}{{\rm d}^2p_T{\rm d}y}\delta(z_0), \tag{5}$$

where $g_q = 2 \times 3$ is the spin and color degeneracy factor, $\tau_i \sim 1/p_T$ is the formation time of the quark or anti-quark jet, and z_0 is its position in the QGP expansion direction. $\mathcal{P}(|\boldsymbol{\omega}_r|)$ is the initial jet production probability distribution at the radial position $\boldsymbol{\omega}_r$ in the plane z_0, where

$$|\boldsymbol{\omega}_r| = \left[\mathbf{r} - (\tau - \tau_i)\frac{\mathbf{p}}{|\mathbf{p}|}\right]\cdot\mathbf{r} = \sqrt{(r\cos\phi - \tau)^2 + r^2\sin^2\phi} \quad \text{for } \tau_i \sim 0 \tag{6}$$

and ϕ is the angle in the plane z_0 between the direction of the virtual photon and the position where this virtual photon has been produced.

Equation (1) can be written as

$$\frac{\mathrm{d}R^{l^+l^-}}{\mathrm{d}^4P} = \frac{5\alpha^2}{72\pi^5}\int\frac{\mathrm{d}^3\mathbf{p}_1}{E_{p_1}}\frac{\mathrm{d}^3\mathbf{p}_2}{E_{p_2}}f_{q/\bar{q}}(\mathbf{p}_1,\xi,p_{\mathrm{hard}})f_{\mathrm{jet}}(\mathbf{p}_2) \times\delta^{(4)}(P-p_1-p_2) = \frac{5\alpha^2}{72\pi^5}\int\frac{\mathrm{d}^3\mathbf{p}_1}{E_{p_1}E_{p_1}}f_{q/\bar{q}}(\mathbf{p}_1,\xi,p_{\mathrm{hard}})f_{\mathrm{jet}}(\mathbf{p}-\mathbf{p}_1) \times\delta(E-E_{p_1}-E_{p_2})\big|_{\mathbf{p}_2=\mathbf{P}-\mathbf{p}_2}. \quad (7)$$

If we choose

$$\mathbf{p}_1 = p_1(\sin\theta_{p_1}\cos\phi_{p_1},\sin\theta_{p_1}\sin\phi_{p_1},\cos\theta_{p_1}), \quad \mathbf{P} = P(\sin\theta_P\cos\phi_P,\sin\theta_P\sin\phi_P,\cos\theta_P) \quad (8)$$

and the anisotropy vector $\hat{\mathbf{n}}$ along the z-direction, the δ function can be expressed as

$$\delta(E-E_{p_1}-E_{p_2}) = 2(E-p_1)\chi^{-1}\Theta(\chi)\sum_i^2\delta(\phi_i-\phi_{p_1}) \quad (9)$$

with $\chi=[4P^2p_1^2\sin^2\theta_P\sin^2\theta_{p_1}-[2p_1(E-P\cos\theta_P\cos\theta_{p_1})-M^2]^2]>0$, and the angle ϕ_i can be found by the solutions of the following equation:

$$\cos(\phi_i-\phi_{p_1}) = \frac{2p_1(E-P\cos\theta_P\cos\theta_{p_1})-M^2}{2Pp_1\sin\theta_P\sin\theta_{p_1}}. \quad (10)$$

Equation (7) can now be written as

$$\frac{\mathrm{d}R^{l^+l^-}}{\mathrm{d}^4P} = \frac{5\alpha^2}{18\pi^5}\int_{-1}^{+1}\mathrm{d}(\cos\theta_{p_1})\int_{a_+}^{a_-}\frac{\mathrm{d}p_1}{\sqrt{\chi}}p_1 \times f_{q/\bar{q}}\left(\sqrt{\mathbf{p}_1^2(1+\xi\cos^2\theta_{p_1})},p_{\mathrm{hard}}\right)f_{\mathrm{jet}}(\mathbf{p}-\mathbf{p}_1) \quad (11)$$

with

$$a_\pm = \frac{M^2}{2[E-P\cos(\theta_P\pm\theta_{p_1})]}. \quad (12)$$

Now, the dilepton production rate R is defined as the total number of lepton pair emitted from the 4-dimensional space-time element $\mathrm{d}^4x=\tau\,\mathrm{d}\tau\,\mathrm{d}\eta\,\mathrm{d}^2x_\perp$ with $R=\mathrm{d}N/\mathrm{d}^4x$. Here, $\tau=\sqrt{t^2-z^2}$ is the longitudinal proper time, $\eta=\tanh^{-1}(z/t)$ is the space-time rapidity, and $\mathbf{x}_\perp$ is a two-vector containing the transverse coordinates.

The total dilepton spectrum is given by a full space-time integration:

$$\frac{\mathrm{d}N^{l^+l^-}}{\mathrm{d}M^2\mathrm{d}y} = \int_{p_T^{\min}}^{p_T^{\max}}\mathrm{d}^2p_T\int_{\tau_i}^{\tau_f}\tau\,\mathrm{d}\tau\int_0^{R_\perp}r\,\mathrm{d}r\int_0^{\pi}\mathrm{d}\phi \times\int_{-\infty}^{+\infty}\mathrm{d}\eta\frac{\mathrm{d}R^{l^+l^-}}{\mathrm{d}^4P}(E=m_T\cosh(y-\eta)) \quad (13)$$

and

$$\frac{\mathrm{d}N^{l^+l^-}}{\mathrm{d}^2p_T\mathrm{d}y} = \int_{M^{\min}}^{M^{\max}}\mathrm{d}M^2\int_{\tau_i}^{\tau_f}\tau\,\mathrm{d}\tau\int_0^{R_\perp}r\,\mathrm{d}r\int_0^{\pi}\mathrm{d}\phi \times\int_{-\infty}^{+\infty}\mathrm{d}\eta\frac{\mathrm{d}R^{l^+l^-}}{\mathrm{d}^4P}(E=m_T\cosh(y-\eta)), \quad (14)$$

where $R_\perp=1.2[\langle N_{\mathrm{part}}\rangle/2]^{1/3}$ is the transverse dimension of the system and m_T is the transverse mass of the pair. We have assumed that the plasma is formed at time τ_i and it undergoes a phase transition at transition temperature (T_c) which begins at the time τ_f. τ_f is obtained by using the condition $p_{\mathrm{hard}}(\tau=\tau_f)=T_c$. The energy of the dilepton pair in the fluid rest frame has to be understood as $E=m_T\cosh(y-\eta)$. Now the ϕ integration can be done as follows:

$$\int_0^{\pi}\mathrm{d}\phi\,\mathcal{P}(|\boldsymbol{\omega}_r|) = \begin{cases} 0, & \text{for } r^2+\tau^2-2\tau r>R_\perp^2,\\ \dfrac{4}{R_\perp^2}\left(1-\dfrac{r^2+\tau^2}{R_\perp^2}\right), & \text{for } r^2+\tau^2+2\tau r<R_\perp^2,\\ \dfrac{4u_0}{\pi R_\perp^2}\left(1-\dfrac{r^2+\tau^2}{R_\perp^2}\right) & \\ \quad+\dfrac{8\tau r}{\pi R_\perp^4}\sin(u_0), & \text{otherwise,}\end{cases} \quad (15)$$

where

$$u_0 = \arccos\left(\frac{r^2+\tau^2-R_\perp^2}{2\tau r}\right). \quad (16)$$

3 Jets production and Drell-Yan process

The differential cross-section for the jet production in hadron-hadron collision ($A+B\to\text{jets}+X$) can be written as [39]

$$\frac{\mathrm{d}\sigma_{\mathrm{jet}}}{\mathrm{d}^2p_T\mathrm{d}y} = K\sum_{a,b}\int_{x_a^{\min}}^1\mathrm{d}x_aG_{a/A}(x_a,Q^2)G_{b/B}(x_b,Q^2) \times\frac{x_ax_b}{x_a-\frac{p_T}{\sqrt{s}}e^y}\frac{1}{\pi}\frac{\mathrm{d}\hat{\sigma}_{ab\to\mathrm{cd}}}{\mathrm{d}\hat{t}}, \quad (17)$$

where $\sqrt{s}$ is the total energy in the center-of-mass and x_a (x_b) is the momentum fraction of the parton a (b) of the nucleon A (B). $G_{a/A}$ ($G_{b/B}$) is the parton distribution function (PDF) of the incoming parton a (b) in the incident hadron A (B). K factor is used to account the next-to-leading (NLO) order effect. The minimum value of x_a is

$$x_a^{\min} = \frac{p_Te^y}{\sqrt{s}-p_Te^{-y}}. \quad (18)$$

The value of the momentum fraction x_b can be written as

$$x_b = \frac{x_ap_Te^{-y}}{x_a\sqrt{s}-p_Te^y}. \quad (19)$$

$\frac{\mathrm{d}\hat{\sigma}_{ab\to\mathrm{cd}}}{\mathrm{d}\hat{t}}$ is the cross section of parton collision at leading order. These process are: $qq\to qq$, $q\bar{q}\to q\bar{q}$, $q\bar{q}\to q'\bar{q}'$, $qq'\to qq'$, $q\bar{q}'\to q\bar{q}'$, $qg\to qg$, and $gg\to q\bar{q}$. The yield for producing jets in the heavy-ion collision is given by

$$\frac{\mathrm{d}N_{\mathrm{jet}}}{\mathrm{d}^2p_T\mathrm{d}y} = T_{\mathrm{AA}}\frac{\mathrm{d}\sigma_{\mathrm{jet}}}{\mathrm{d}^2p_T\mathrm{d}y}\bigg|_{y=0}, \quad (20)$$

where $T_{\rm AA} = 9A^2/8\pi R_\perp^2$ is the nuclear thickness function for zero impact parameter [38]. The p_T distribution of the jet quarks in the central rapidity region ($y = 0$) was computed in [12] and parameterized as

$$\left.\frac{{\rm d}N_{\rm jet}}{{\rm d}^2p_T{\rm d}y}\right|_{y=0} = K\frac{a}{(1+\frac{p_T}{b})^c}\,. \tag{21}$$

Numerical values for the parameters a, b and c are listed in ref. [12].

The cross-section for the Drell-Yan process (LO) is given by [10]

$$\begin{aligned}\frac{{\rm d}N_{\rm DY}}{{\rm d}M^2{\rm d}y} &= T_{\rm AA}K_{\rm DY}\frac{4\pi\alpha^2}{9M^4}\\ &\times\sum_q e_q^2\big[x_1G_{q/A}(x_1,Q^2)x_2G_{\bar q/B}(x_2,Q^2)\\ &+x_1G_{\bar q/A}(x_1,Q^2)x_2G_{q/B}(x_2,Q^2)\big],\end{aligned} \tag{22}$$

where the momentum fractions with rapidity y are $x_1 = \frac{M}{\sqrt{s}}e^y$, $x_2 = \frac{M}{\sqrt{s}}e^{-y}$. $K_{\rm DY}$ factor of 1.5 is used to account for the NLO correction [40]. We have used the CTEQ6 parton distribution functions for our calculations [41].

It should be noted that we have not included the shadowing effect in our calculation. Inclusion of this effect will reduce the Drell-Yan contribution leaving a more promising window for the jet-dilepton contribution. It is worthwhile to mention that the gluon saturation effect has not been included in our calculation as recent experimental results show that there is no significant change in the gluon distribution function of the proton for Bjorken-x between 2×10^{-02} to 2×10^{-05} from HERA to LHC energies [42].

4 Space-time evaluation

For the case of expanding plasma, we will be required to specify a proper-time dependence of the anisotropy parameter, ξ and the hard momentum scale, $p_{\rm hard}$. In our calculation, we assume an isotropic plasma is formed at initial time τ_i and initial temperature T_i. The initial rapid expansion of the matter along the longitudinal direction causes faster cooling in this direction than in the transverse direction [18] and as result, a local momentum-space anisotropy occurs and remains until $\tau = \tau_{\rm iso}$. In this work, we shall follow the work of ref. [31, 34] to evaluate the dilepton production rate from the first few Fermi of the plasma evolution. According to this model there can be three possible scenarios: i) $\tau_i = \tau_{\rm iso}$, the system evolves hydrodynamically so that $\xi(\tau) = 0$ and we can identify the hard momentum scale with the plasma temperature so that $p_{\rm hard}(\tau) = T(\tau) = T_0(\tau_i/\tau)^{1/3}$, ii) $\tau_{\rm iso}\to\infty$, the system never comes to equilibrium, iii) $\tau_{iso}\geq\tau_i$ and $\tau_{\rm iso}$ is finite, one should devise a time evolution model for $\xi(\tau)$ and $p_{\rm hard}(\tau)$ which smoothly interpolates between pre-equilibrium anisotropy and hydrodynamics and we shall follow scenario iii). The time dependent parameters ξ and $p_{\rm hard}$ are obtained in terms of a smeared step function [34]:

$$\lambda(\tau) = \frac{1}{2}(\tanh[\gamma(\tau-\tau_{iso})/\tau_i]+1), \tag{23}$$

where the transition width, γ^{-1} is introduced to take into account the smooth transition between non-equilibrium and hydrodynamical evolution at $\tau = \tau_{\rm iso}$. It is clearly seen that for $\tau\ll\tau_{\rm iso}$, we have $\lambda\to0$, corresponding to anisotropic evolution and for $\tau\gg\tau_{\rm iso}$, $\lambda\to1$ which corresponds to hydrodynamical evolution.

With this, the time dependence of relevant quantities are as follows [31,34]:

$$\begin{aligned}p_{\rm hard}(\tau) &= T_i\ [\mathcal{U}(\tau)/\mathcal{U}(\tau_i)]^{1/3}\\ \text{and}\quad \xi(\tau) &= a^{\delta[1-\lambda(\tau)]}-1,\end{aligned} \tag{24}$$

where $\mathcal{U}(\tau)\equiv[\mathcal{R}(a_{\rm iso}^\delta-1)]^{3\lambda(\tau)/4}(a_{\rm iso}/a)^{1-\delta[1-\lambda(\tau)]/2}$, $a\equiv\tau/\tau_i$ and $a_{\rm iso}\equiv\tau_{\rm iso}/\tau_i$ and $\mathcal{R}(x) = \frac{1}{2}(\frac{1}{1+\xi}+\frac{\arctan\sqrt{\xi}}{\sqrt{\xi}})$. In the present work, we have used a *free streaming interpolating* model that interpolates between early-time $(1+1)$-dimensional longitudinal free streaming and late-time $(1+1)$-dimensional ideal hydrodynamic expansion by choosing $\delta = 2$.

As the colliding nuclei do have a transverse density profile, we assume that the initial temperature profile is given by [43]

$$T_i(r) = T_i\ \left[2\left(1-r^2/R_A^2\right)\right]^{1/4}. \tag{25}$$

Using eqs. (24) and (25) we obtain the profile of the hard momentum scale as

$$p_{\rm hard}(\tau,r) = T_i\ \left[2\left(1-r^2/R_A^2\right)\right]^{1/4}\bar{\mathcal{U}}^{c_s^2}(\tau). \tag{26}$$

In case of isentropic expansion the initial temperature (T_i) and thermalization time (τ_i) can be related to the observed particle rapidity density by the following equation [44]:

$$T_i^3(b_m)\tau_i = \frac{2\pi^4}{45\zeta(3)}\frac{1}{\pi R_\perp}\frac{1}{4a_k}\left\langle\frac{{\rm d}N}{{\rm d}y}(b_m)\right\rangle, \tag{27}$$

where $\frac{{\rm d}N}{{\rm d}y}(b_m)$ is the hadron multiplicity for a given centrality class with maximum impact parameter b_m, $R_\perp$ is the transverse dimension of the system, $\zeta(3)$ is the Riemann zeta function, and $a_k = (\pi^2/90)g_k$ for a plasma of massless u, d and s quarks and gluons, where $g_k = 42.25$.

5 Results

The hadron multiplicity resulting from Au + Au collisions is related to that from pp collision at a given impact parameter and collision energy by

$$\left\langle\frac{{\rm d}N}{{\rm d}y}(b_m)\right\rangle = [(1-x)\,\langle N_{part}(b_m)\rangle/2 + x\langle N_{coll}(b_m)\rangle]\,\frac{{\rm d}N_{pp}}{{\rm d}y}\,, \tag{28}$$

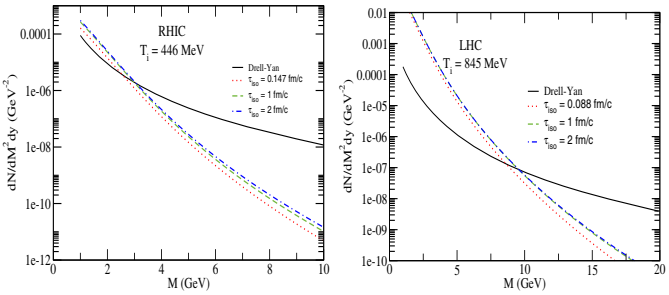

Fig. 1. Dilepton yield for central Au + Au collisions at $\sqrt{S_{NN}} = 200\,\text{GeV}$ (left panel) and for central Pb + Pb collisions at $\sqrt{S_{NN}} = 5.5\,\text{TeV}$ (right panel).

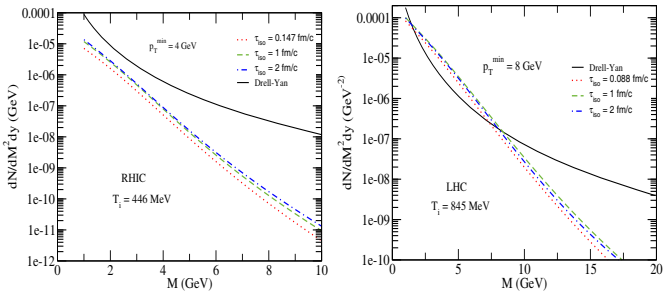

Fig. 2. Dilepton yield for central Au + Au collisions at $\sqrt{S_{NN}} = 200\,\text{GeV}$ (left panel) and for central Pb + Pb collisions at $\sqrt{S_{NN}} = 5.5\,\text{TeV}$ (right panel).

where x is the fraction of hard collisions. $\langle N_{part}\rangle$ is the average number of participants and $\langle N_{coll}\rangle$ is the average number of collisions evaluated by using Glauber model. $\mathrm{d}N_{pp}^{ch}/\mathrm{d}y = 2.5 - 0.25\ln(s) + 0.023\ln^2 s$ is the multiplicity of the produced hadrons in pp collisions [45] at center of mass energy, $\sqrt{s}$ scaled by nucleon mass taken as $\sim 1\,\text{GeV}$. We have assumed that 20% hard (*i.e.* $x = 0.20$) and 80% soft collisions are responsible for initial entropy production. This gives the desired multiplicity measured at RHIC energies. For 0–10% centrality we obtain $T_i = 446\,\text{MeV}$ for $\tau_i = 0.147\,\text{fm/c}$. Following the same methodology, for LHC energies ($\sqrt{s} = 5.5\,\text{TeV}$), we find the initial conditions as $T_i = 845\,\text{MeV}$ with $\tau_i = 0.088\,\text{fm/c}$.

For anisotropic hydrodynamics the time τ_f at which the quark gluon plasma phase ends depends upon the values of T_i, τ_i and τ_{iso}. Thus for initial conditions corresponding to RHIC energies we have the following values of τ_f. $\tau_f = 2.65, 3.6, 4.26\,\text{fm/c}$ for $\tau_{\text{iso}} = 0.147, 1, 2\,\text{fm/c}$, respectively. At LHC energies, $\tau_f = 10.81, 16.6, 19.7\,\text{fm/c}$ for $\tau_{\text{iso}} = 0.088, 1, 2\,\text{fm/c}$, respectively. We take the transition temperature $T_c \sim 170\,\text{MeV}$.

Using the above initial conditions, we display the invariant mass distribution for RHIC (left panel) and LHC (right panel) energies in fig. 1. We have used $p_T^{\min} = 2\,\text{GeV}$. It is found that the contribution from jet-dilepton conversion in isotropic plasma dominates over the Drell-Yan contribution up to $M \sim 2.5\,\text{GeV}$ (see left panel). However, when anisotropy is introduced this threshold increases to $M = 3\,\text{GeV}$ irrespective of the values of the isotropization time. For LHC energies (right panel) this threshold increases up to $M \sim 10\,\text{GeV}$ providing an expanded window at LHC where jet-conversion dilepton could be observed when initial momentum-space anisotropy is taken into account. However, the dominance of the jet-dilepton conversion over the Drell-Yan contribution is sensitive to the choice of $p_T^{\min}$. In case of $p_T^{\min} = 4\,\text{GeV}$ for RHIC energies, even if we introduce initial momentum-space anisotropy, we find that the two contributions do not intersect for any value of M. On the other hand, including the anisotropy effect for LHC energies with $p_T^{\min} = 8\,\text{GeV}$, we observe a comparatively larger window in M for which the jet-dilepton conversion contribution dominates compared to the isotropic case as shown in fig. 2.

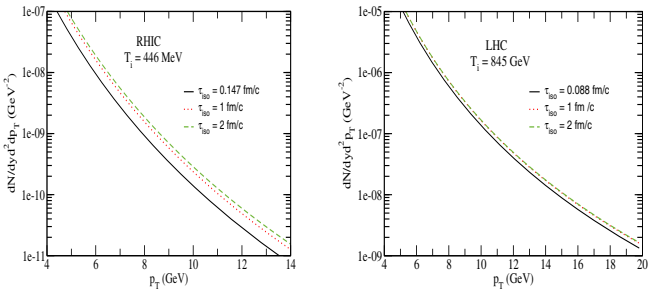

Fig. 3. p_T distribution of the jet-conversion dilepton, integrated in the range $0.5\,\text{GeV} < M < 1\,\text{GeV}$, for the RHIC (left panel) and the LHC (right panel).

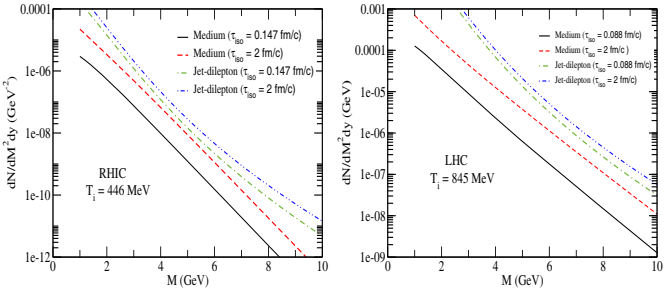

Fig. 4. Collisionally broadened interpolating model dilepton yield and jet-conversion dilepton yield as a function of invariant mass in central Au + Au collisions at $\sqrt{S_{NN}} = 200\,\text{GeV}$ (left panel) and for central Pb + Pb collisions at $\sqrt{S_{NN}} = 5.5\,\text{TeV}$ (right panel).

The p_T-distribution is shown in fig. 3 where we find that the effect of anisotropy at RHIC energies is substantial (increases by a factor of 4). Surprisingly, at LHC energies the effect is not substantial. In fig. 4 we compare the contribution from jet-dilepton conversion with the medium dilepton [31], where $f_{\text{jet}}(\mathbf{p}_2)$ in eq. (1) is replaced by $f_{\bar{q}/q}(\mathbf{p}_2)$. It is shown that in case of $\tau_{iso} = 0.147\,\text{fm/c}$ $(0.088\,\text{fm/c})$ for RHIC (LHC) which corresponds to isotropic momentum space distribution, the jet-dilepton contribution exceeds the thermal dilepton production by an order of magnitude which is consistent with ref. [13]. For both the energies, with the introduction of initial state anisotropy, the medium dilepton yield increases with respect to the isotropic case as found in ref. [31,34]. In our work we find that jet-dilepton

contribution coming from the interaction between jet and AQGP is in fact an order of magnitude larger in comparison to the isotropic jet-dilepton conversion as well as anisotropic medium contribution for both RHIC and LHC energies. However, here also the dependence on $p_T^{\min}$ can not be neglected. It has been observed that in low invariant mass region with $p_T^{\min} = 1\,\text{GeV}$, medium dilepton production rate dominates over the jet-medium dilepton production rate even for the AQGP.

Few comments about the initial conditions are in order here. For model calculations of various observables at RHIC and LHC energies one can vary the initial conditions (such as T_i by varying τ_i) and the initial temperature usually lies in the range of $T_i \sim 350$–$440\,\text{MeV}$ for RHIC [46–49]. For example, in [15], T_i for RHIC is assumed to be $\sim 370\,\text{MeV}$ in which case the jet-dilepton contribution remains above the DY lepton pair up to $M \sim 3\,\text{GeV}$ which is similar to our case although the initial temperature is higher. In the same work the initial temperature for LHC energies is taken as $T_i \sim 845\,\text{MeV}$ which is similar to our case.

6 Summary and discussion

In this work we have calculated the contribution of lepton pair production in the high-mass region from jet-plasma interactions in AQGP. For simplicity, (1 + 1)d anisotropic hydrodynamics has been used as the effect of transverse expansion will be marginal in the early stage of the collision (note that momentum-space anisotropy is an early time phenomenon). It is found that the threshold value of M beyond which DY process dominates over jet-conversion dilepton increases marginally with the introduction of momentum-space anisotropy both for RHIC and LHC. However, we do not find any appreciable change in the p_T distribution at LHC energies even if the anisotropy is introduced. We have also shown that the medium dilepton contribution always remains below the dilepton from the jet plasma interaction. In fact, the former is less by a factor 4–10 depending upon τ_{iso} and p_T. Since we are considering the high-mass lepton pair, the contributions from $q\bar{q}$ annihilation (isotropic) as well as hadronic matter will be subleading there. Lepton pair from hadronic reactions and decays usually dominates in the intermediate mass region. Moreover, as the radial flow is not developed properly in the initial stage of the collision, its effect is neglected here [50]. It should also be noted that a different initial temperature could be obtained by varying τ_i. The chosen set for RHIC energies gives the best fit of other experimental observables [33,35]. Finally, in the present calculation we have not included the energy loss of the energetic jets which we propose to report elsewhere [51].

References

1. J. Kapusta, P. Lichard, D. Seibert, Phys. Rev. D **44**, 2774 (1991) **47**, 4171(E) (1993).
2. R. Baier, H. Nakkagawa, A. Niegawa, K. Redlich, Z. Phys. C **53**, 433 (1992).
3. P.K. Roy, D. Pal, S. Sarkar, D.K. Srivastava, B. Sinha, Phys. Rev. C **53**, 2364 (1996).
4. P. Aurenche, F. Gelis, H. Zaraket, R. Kobes, Phys. Rev. D **58**, 085003 (1998).
5. P. Arnold, G.D. Moore, L.G. Yaffe, JHEP **12**, 009 (2001).
6. K. Kajantie, J. Kapusta, L. Mclerran, A. Mekjian, Phys. Rev. D **34**, 2746 (1986).
7. K.J. Eskola, J. Lindfors, Z. Phys. C **46**, 141 (1990).
8. K. Geiger, J.I. Kapusta, Phys. Rev. Lett. **70**, 1920 (1993).
9. B. Kampfer, O.P. Pavlenko, Nucl. Phys. A **566**, 351 (1994).
10. E.V. Shuryak, Phys. Lett. B **78**, 150 (1978).
11. M. Strickland, Phys. Lett. B **331**, 245 (1994).
12. D.K. Srivastava, C. Gale, R.J. Fries, Phys. Rev. C **67**, 034903 (2003).
13. S. Turbide, C. Gale, D.K. Srivastava, R.J. Fries, Phys. Rev. C **74**, 014903 (2006).
14. Yong-Ping Fu, Yun-De Li, Nucl. Phys. A **865**, 76 (2011).
15. Yong-Ping Fu, Q. Xi, Phys. Rev. C **92**, 024914 (2015).
16. S.D. Drell, T.M. Yan, Phys. Rev. Lett. **25**, 316 (1970).
17. P. Huovinen, P.F. Kolb, U.W. Heinz, P.V. Ruuskanen, S.A. Voloshin, Phys. Lett. B **503**, 58 (2001).
18. R. Baier, A.H. Mueller, D. Schiff, D.T. Son, Phys. Lett. B **502**, 51 (2001).
19. Z. Xu, C. Greiner, Phys. Rev. C **71**, 064901 (2005).
20. M. Strickland, J. Phys. G **34**, S429 (2007).
21. M. Luzum, P. Romatschke, Phys. Rev. C **78**, 034915 (2008) **79**, 039903(E) (2009).
22. S. Mrowczynski, M.H. Thoma, Phys. Rev. D **62**, 036011 (2000).
23. P. Romatschke, M. Strickland, Phys. Rev. D **68**, 036004 (2003).
24. P. Romatschke, M. Strickland, Phys. Rev. D **70**, 116006 (2004).
25. P. Arnold, J. Lenaghan, G.D. Moore, JHEP **08**, 002 (2003).
26. S. Mrowczynski, A. Rebhan, M. Strickland, Phys. Rev. D **70**, 025004 (2004).
27. A. Rebhan, P. Romatschke, M. Strickland, Phys. Rev. Lett. **94**, 102303 (2005).
28. P. Arnold, G.D. Moore, L.G. Yaffe, Phys. Rev. D **72**, 054003 (2005).
29. B. Schenke, M. Strickland, C. Greiner, M.H. Thoma, Phys. Rev. D **73**, 125004 (2006).
30. M. Mandal, P. Roy, Adv. High Energy Phys. **2013**, 371908 (2013).
31. M. Martinez, M. Strickland, Phys. Rev. C **78**, 034917 (2008).
32. L. Bhattacharya, P. Roy, J. Phys. G **37**, 105010 (2010).
33. L. Bhattacharya, P. Roy, Phys. Rev. C **79**, 054910 (2009).
34. M. Martinez, M. Strickland, Phys. Rev. Lett. **100**, 102301 (2008).
35. M. Mandal, L. Bhattacharya, P. Roy, Phys. Rev. C **84**, 044910 (2011).
36. J.I. Kapusta, L.D. McLerran, D.K. Srivastava, Phys. Lett. B **283**, 145 (1992).
37. A. Dumitru, D.H. Rischke, T. Schonfeld, L. Winckelmann, H. Stocker, W. Greiner, Phys. Rev. Lett. **70**, 2860 (1993).
38. R.J. Fries, B. Muller, D.K. Srivastava, Phys. Rev. Lett. **90**, 132301 (2003).
39. J.F. Owens, Rev. Mod. Phys. **59**, 465 (1987).
40. R. Rapp, E.V. Shuryak, Phys. Lett. B **473**, 13 (2000).

41. S. Kretzer, H.L. Lai, F.I. Olness, W.K. Tung, Phys. Rev. D **69**, 114005 (2004).
42. ALICE Collaboration (B. Abelev *et al.*), Phys. Rev. Lett. **113**, 232504 (2014).
43. S. Turbide, C. Gale, S. Jeon, G.D. Moore, Phys. Rev. C **72**, 014906 (2005).
44. R.C. Hwa, K. Kajantie, Phys. Rev. D **32**, 1109 (1985).
45. D. Khazreev, M. Nardi, Phys. Lett. B **507**, 121 (2001).
46. Y.-P. Fu, Q. Xi, Commun. Theor. Phys. **66**, 681 (2016).
47. W. Florkowski, *Phenomenology of Ultra-relativistic Heavy-ion Collisions* (World Scientific, Singapore, 2010).
48. R.S. Bhalerao, arXiv:1404.3294v1 [nucl-th].
49. P.F. Kolb, U. Heinz, arXiv:nucl-th/0305084.
50. D.K. Srivastava, M.G. Mustafa, B. Muller, Phys. Rev. C **56**, 1064 (1997).
51. A. Mukherjee *et al.*, in preparation.